ELSEVIER

Journal of Power Sources 76 (1998) 147–152

JOURNAL OF POWER SOURCES

Electrochemical intercalation of cationic and anionic species from a lithium perchlorate–propylene carbonate system—a rocking-chair type of dual-intercalation system

R. Santhanam *, M. Noel

Central Electrochemical Research Institute, Karaikudi 630006, India

Received 3 July 1998; accepted 17 August 1998

Abstract

The reductive and oxidative intercalation of ionic species of lithium perchlorate ($LiClO_4$) in propylene carbonate (PC) medium are carried out to develop a dual-intercalation battery system. Cyclic voltammetry (CV), potentiostatic transients (i-t), galvanostatic charging, thermogravimetry (TG) and differential thermal analysis (DTA) are performed to establish the intercalation behaviour of both lithium and perchlorate ionic species. A polypropylene graphite composite electrode material containing 20 wt.% polypropylene as a binder is found to be a suitable host material for dual intercalation studies. The intercalation/de-intercalation efficiency (IDE) increases with increasing sweep rate and reaches up to 90% for Li^+ and 65% for ClO_4^- ions at a sweep rate of 40 mV s^{-1}. The formation of a passive film decreases the IDE during the first intercalation/de-intercalation cycle. The open-circuit potential for a battery assembly involving these two electrodes is in the range 3.8 to 4.0 V.

Keywords: Graphite electrodes; Lithium-ion batteries; Intercalation

1. Introduction

Lithium-ion batteries have been the subject of substantial research and a development throughout the world. In conventional lithium-ion batteries the negative electrode (anode) is a Li–C intercalation compound and the positive electrode (cathode) is based on a transition metal oxide such as NiO_2, CoO_2 or Mn_2O_4 [1]. Lithium-ion batteries are more attractive because their specific energies are two- to three-times higher than those of nickel–metal hydride (Ni–MH) or nickel–cadmium (Ni–Cd) batteries. The use of graphite provides improvements such as safety, reliability, environmental friendliness, and economy. The transition metal oxides, on the other hand, are expensive, less desirable environmentally and more synthetically demanding than either carbon or graphite. Hence, it is necessary to optimize further the existing battery design and performance and through, for example, the identification and characterization of new rocking-chair cell materials and configurations.

It is well-known that a number of cations as well as anions can be reversibly intercalated into graphite electrodes using appropriate solvent-supporting electrolyte systems [2–13]. Nevertheless, simultaneous intercalation of both anions and cations into graphite electrodes from a single solvent-supporting electrolyte system has still to be accomplished. By contrast, dual-intercalating molten electrolyte battery systems which involve organic salts and anode and cathode electrodes made from graphite have been reported [14]. In a previous publication [15], we have reported a potential dual-intercalation battery system in which a tetrabutylammonium perchlorate–propylene carbonate system was used for simultaneous intercalation of both tetrabutylammonium ion and perchlorate ion. Recently, a new type of rocking chair battery family based on a graphite negative electrode and a polymer positive electrode has been demonstrated [16]. During intercalation/de-intercalation of ionic species into graphite, the surface damage caused by the large tetrabutylammonium cation (TBA^+) is more than with the smaller lithium cation (Li^+) [17]. An improved intercalation/de-intercalation efficiency (IDE) has been obtained in the present work when lithium perchlorate–propylene carbonate ($LiClO_4$–PC) is used as the solvent-supporting elecrolyte system.

* Corresponding author. Fax: +91-4565-22088; E-mail: cecrik@cscecri.ern.nic.in

0378-7753/98/$19.00
PII: S0378-7753(98)00152-9

2. Experimental

A polypropylene graphite composite (CPP) rod of 3 mm diameter and that contained 80% natural graphite and 20% polypropylene as a binder embedded in a Teflon rod was employed as a working electrode, together with a platinum counter electrode and a saturated calomel reference electrode. Analar grade distilled propylene carbonate and Analar grade dried lithium perchlorate were used throughout the work. The working electrode was polished thoroughly with 1/0 to 5/0 emery papers. The electrochemical reversibility of the working electrode was evaluated using a 2 mM ferricyanide solution (Ep = 65 mV) in 0.1 M potassium chloride.

Cyclic voltammograms and chronoamperograms were obtained with a potentiostat (Wenking Model LB 75 M, Germany), a voltage scan generator (Wenking Model VSG 72) and a recorder (Rikadenki Model RW-201T). Thermogravimetry (TG) and differential thermal analysis (DTA) were carried out by means of a computer-controlled thermal analyser (Model STA 1500, PL Thermal Sciences, UK).

3. Results and discussion

3.1. Cyclic voltammetric studies

3.1.1. Effect of passive film formation

Typical cyclic voltammograms (sweep rate = 40 mV s^{-1}) obtained for cathodic Li^+ ion and for anodic ClO_4^- ion intercalation/de-intercalation processes in a PC medium with 0.25 M $LiClO_4$ are shown in Fig. 1. The first cycle of the intercalation/de-intercalation process of Li^+ and ClO_4^- ions is shown in Fig. 1a and b, respectively. The second and subsequent cycles are shown in Fig. 1c and d, respectively. For Li^+ ions, the charge recovery ratio (Qdi/Qin), or intercalation/de-intercalation efficiency (IDE), is 45.6% on the first cycle and 63.9% on the second. For ClO_4^- ions, an IDE of 34.6% and 53.9% is obtained on the first and second cycle, respectively. This difference in IDE on the first and second intercalation/de-intercalation cycle is due to competitive processes, namely, passive film formation and solvent decomposition. The competitive processes predominate over the intercalation process during the first charge/discharge cycle. Hence, the IDE is less on the first cycle than on the second cycle. The intercalation reaction appears to proceed smoothly without further decomposition of the solvent through the passive film from the second cycle onwards. This type of passivating layer on graphite in alkyl carbonate solution has been reported and characterized recently by Mori et al. [18] and Aurbach et al. [19].

3.1.2. Effect of multi-sweep cyclic voltammetry

The intercalation/de-intercalation process is generally found to be quite reversible and can be repeated a number of times under identical experimental conditions [12,20,21]. The CPP electrode exhibits good reversibility during intercalation/de-intercalation of Li^+ and ClO_4^- ions on multiple cycling. Typical multi-sweep voltammograms (5 cycles) recorded for the reductive Li^+ and the oxidative ClO_4^- ion intercalation/de-intercalation process are pre-

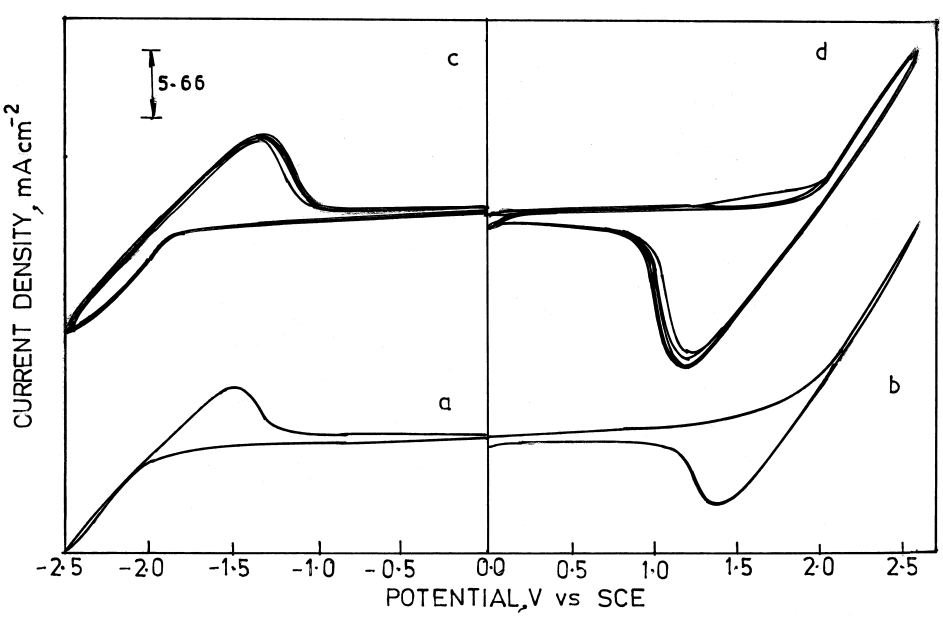

Fig. 1. Cyclic voltammograms for 0.25 M $LiClO_4$ in PC medium with CPP graphite: (a), (c) reductive intercalation of Li^+ ions; (b), (d) oxidative intercalation of ClO_4^- ions; (a), (b) represents first cycle; (c), (d) represents second and subsequent cycles. Sweep rate = 40 mV s^{-1}.

sented in Fig. 1c and d, respectively. The reversibility is close to 100% for both processes. For lithium ions, the cathodic and anodic charges increase slightly with sweep number (Fig. 1c). For ClO_4^- ions, the anodic charge does not increase with sweep number while the cathodic charge increases slightly (Fig. 1d).

3.1.3. Effect of sweep rate

Typical cyclic voltammograms were recorded at different sweep rates from 1 to 40 mV s^{-1} for the intercalation/de-intercalation process of both Li^+ and ClO_4^- ionic species in PC medium with 0.25 M $LiClO_4$. The intercalation charge (Qin), de-intercalation charge (Qdi), intercalation/de-intercalation efficiency (IDE) and de-intercalation peak potential (DPP) obtained at different sweep rates are listed in Table 1. The main reasons for the irreversibility in the intercalation/de-intercalation process are the slow surface transformations and co-intercalation of solvent and its subsequent reduction to form an insulating film within the graphite structure [21]. At short time scales or high sweep rates, the destruction of the graphite structure is believed to be minimum and hence the IDE is expected to be a higher. This is indeed found to be the case for the intercalation/de-intercalation behaviour of both Li^+ and ClO_4^- ions in PC medium. For example, the IDE for Li^+-ion intercalation increases from 15 to 89.5% and for ClO_4^--ion intercalation from 34.4 to 65.4% at 1 and 40 mV s^{-1}, respectively.

An interesting correlation is found to exist between the DPP and the IDE (Fig. 2) at different sweep rates. For Li^+ cations, the DPP varies significantly with sweep rate. For ClO_4^- ions, by comparison, the change in DDP is small with sweep rates. A broad de-intercalation peak covering a wide potential range with more positive DPPs for cations and more negative DPPs for anions naturally leads to higher Qdi and hence higher IDE [12]. Here, the DPP values for both Li^+ and ClO_4^- ions at different sweep rates became more positive and more negative, respectively. Hence, the IDE is greater at higher sweep rates.

Table 1
Cyclic voltammetry data for intercalation and de-intercalation processes on CPP electrode in 0.25 M $LiClO_4$–PC solution at different sweep rates

Ion	Sweep rate (mV s^{-1})	Qin (mC cm^{-2})	Qdi (mC cm^{-2})	IDE (%)	DPP (V)
Li^+	1	2264.0	339.6	15.0	−1.66
	5	713.2	305.6	42.9	−1.50
	10	398.6	254.7	63.9	−1.40
	20	211.4	161.3	76.3	−1.34
	40	104.0	93.1	89.5	−1.30
ClO_4^-	1	8546.6	2943.2	34.4	1.36
	5	1929.9	944.6	49.0	1.24
	10	1013.0	546.0	53.9	1.22
	20	379.2	240.6	63.5	1.18
	40	184.0	120.3	65.4	1.14

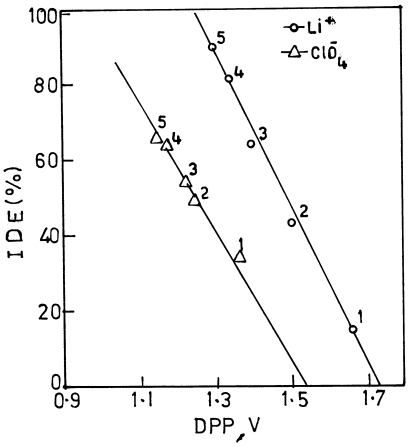

Fig. 2. Li^+ and ClO_4^- ions intercalation/de-intercalation efficiency vs. de-intercalation peak potential of 0.25 M $LiClO_4$ in PC medium with CPP graphite at sweep rates (1) 1, (2) 5, (3) 10, (4) 20 and (5) 40 mV s^{-1}.

3.2. Potentiostatic current-time transients (i-t)

The intercalation/de-intercalation behaviour of Li^+ and ClO_4^- ionic species from PC medium with 0.25 M $LiClO_4$ was evaluated by means of potentiostatic i-t transient measurements (Fig. 3). For Li^+ and ClO_4^- ionic species, the intercalation was carried out at −2.5 and +2.5 V, while de-intercalation was performed at −1.3 and +1.2 V, respectively. All the intercalation and de-intercalation processes were conducted at a constant period of 60 s. The values for Qin, Qdi and IDE for both Li^+ and ClO_4^- ionic

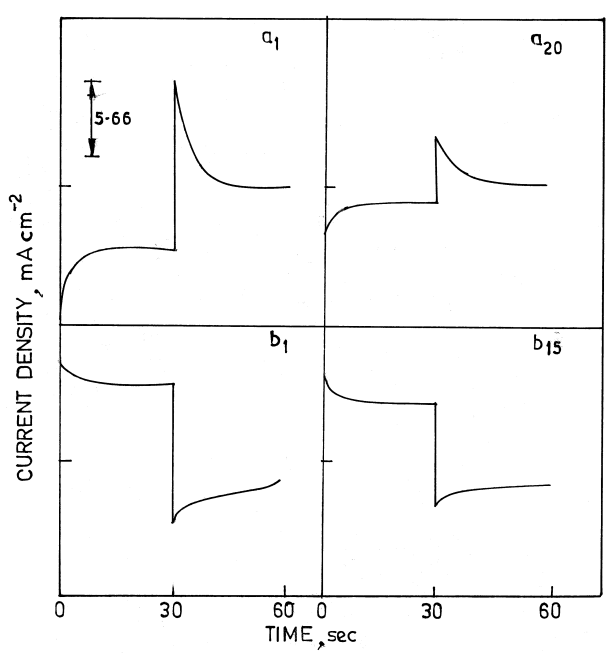

Fig. 3. Double potential step (i-t) transients of CPP electrode in 0.25 M $LiClO_4$–PC solutions. Step time: 1 min; (a) Li^+ intercalation and de-intercalation; (b) ClO_4^- intercalation and de-intercalation. Number of cycles, as indicated.

Table 2
Intercalation and de-intercalation charges and their ratios from current-time measurements in 0.25 M $LiClO_4$–PC solution at different cycle numbers

Ion	Cycle number	Qin (mC cm^{-2})	Qdi (mC cm^{-2})	IDE (%)
Li^+	1	305.6	48.1	15.7
	5	198.1	56.6	28.6
	10	141.5	42.5	30.0
	15	107.5	39.6	36.8
	20	73.6	36.8	50.0
	25	60.6	28.1	46.4
ClO_4^-	1	848.4	424.2	50.0
	5	722.2	396.4	54.9
	10	636.3	353.5	55.6
	15	500.0	285.0	57.0
	20	382.4	152.9	40.0

Table 3
Open-circuit potential from simultaneous intercalation of cations and anions of $LiClO_4$ in PC medium on CPP electrode at different current densities

Time (min)	Open-circuit potential (V)	
	3 mA cm^{-2}	10 mA cm^{-2}
1	3.8	4.0
10	3.5	3.0
20	2.9	2.5
30	2.3	2.1
40	2.0	1.8
50	1.8	1.4
60	1.8	1.4
70	1.8	1.4
80	1.6	1.2
90	1.3	0.8
100	1.0	0.7

Charging time ± 1 h; area of the electrode = 1 cm^2.

species are summarized in Table 2. The IDE increases with increasing cycle number up to 20 cycles for Li^+ ions. After that, the IDE decreases from 50 to 46.4% at the 25th cycle. For ClO_4^- ions, the IDE increases up to 15 cycles and then decreases to 40% at the 20th cycle. It thus appears that in the compact polypropylene graphite material employed here the irreversible surface change sets in beyond 20 and 15 cycles for cation and anion intercalation, respectively. The cycle life can, however, be substantially different on a porous graphite composite material.

3.3. Constant-current charging

Intercalation and de-intercalation processes are primarily investigated for potential battery applications. Hence, long-time charging behaviour at either constant-voltage conditions or constant-current conditions becomes quite important. Here, some preliminary studies relating to the overall discharge behaviour of the $LiClO_4$–PC dual intercalation system have been carried out. For these studies, two electrodes with the same surface area (1 cm^2) were galvanostatically charged at two different current densities. The current densities for charging were selected from cyclic voltammetric curves. The electrode assembly was charged for a constant period of 1 h. The open-circuit potential (OCP) decay was monitored for the subsequent 100 min. Typical OCP decay responses are summarized in Table 3 and graphically displayed in Fig. 4. In the $LiClO_4$–PC dual-intercalation system, the OCP values decrease sharply and stabilize around 1.8 V at low current density and at 1.4 V at high current density. Further investigations on the stability of this interesting dual-intercalation system would be worthwhile.

3.4. Thermogravimetry and differential thermal analysis

The thermal properties of both Li^+-cation and ClO_4^--anion intercalated graphite samples were examined by thermogravimetry (TG) and differential thermal analysis (DTA). The TG and DTA curves of the Li^+-ion intercalated graphite sample are given in Fig. 5a. At 25 to 90°C, a weight decrease up to about 7% and a few small endothermic peaks were observed. The main process is believed to be the evaporation of solvent, namely, propylene carbonate, from the surface of the Li^+-ion intercalated graphite sample. Above 200°C, the 20% decrease in weight and two well-defined exothermic peaks at 205 and 315°C are due mainly to the de-intercalation of the co-intercalated solvent from the interior of the graphite lattice. The TG and DTA curves for a ClO_4^--ion intercalated graphite sample are shown in Fig. 5b. At 50 to 125°C, a rapid weight decrease up to about 25% and a few endothermic peaks are due to the evaporation of the solvent from the surface of the intercalated sample. The weight decrease up to about 20%

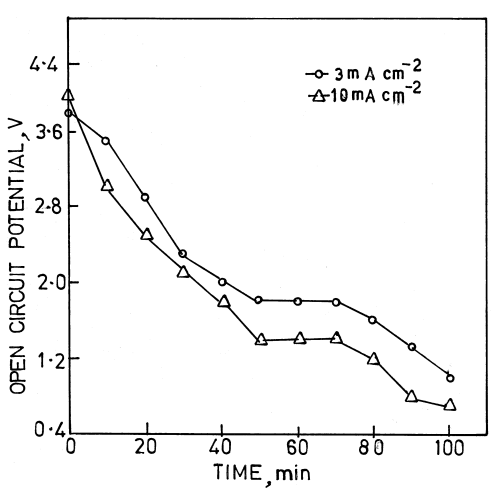

Fig. 4. Open-circuit potential decay of CPP electrode after constant-current charging for 1 h at different current densities in 0.25 M $LiClO_4$–PC solution.

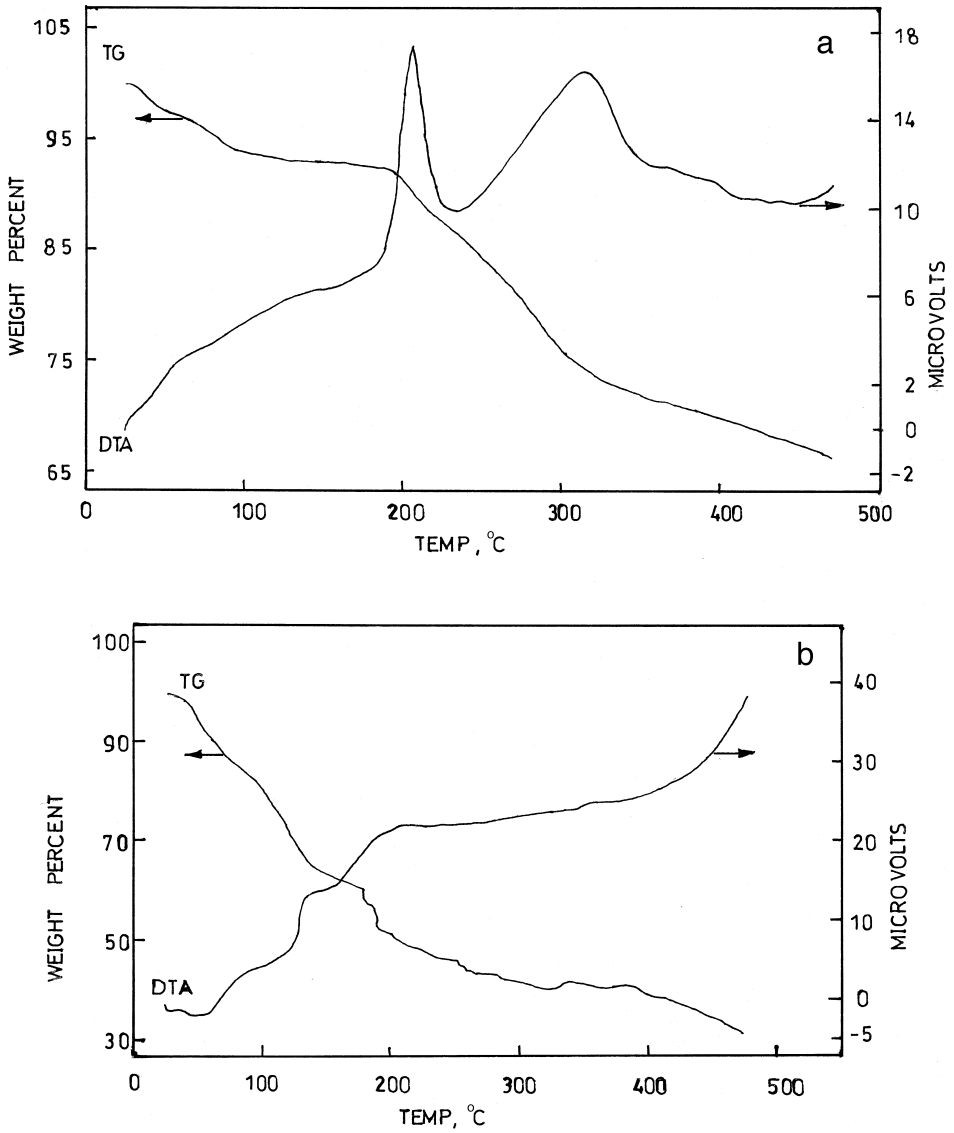

Fig. 5. TG and DTA curves of CPP electrode electrolysed cathodically for 1 h in 0.25 M $LiClO_4$–PC solution at (a) −2.5 V and (b) +2.5 V temperature rise = 5°C min^{-1}.

between 200 and 300°C and some exothermic peaks are mainly attributed to the decomposition of the solvent from the interior surface of the ClO_4^--ion intercalated sample.

3.5. Proposed reactions for dual-intercalation system

For the graphite anode, the charge–discharge process involves the intercalation/de-intercalation of Li^+ ions, i.e.,

$$nC + Li^+ + e \longleftrightarrow C_n^- Li^+$$

while the equivalent charge promotes the intercalation of ClO_4^- ions in the graphite cathode, i.e.,

$$xC + ClO_4^- \longleftrightarrow C_x^+ ClO_4^- + e$$

The overall process is:

$$(n + x)C + LiClO_4 \longleftrightarrow C_n^- Li^+ + C_x^+ ClO_4^-$$

4. Conclusions

The following conclusions may be drawn from the present investigation: (i) inexpensive graphite electrodes can be used for both the anode as well as the cathode; (ii) a single solvent-supporting electrolyte system (PC–$LiClO_4$) can be used at room temperature to provide the intercalating ions for a graphite anode and cathode; (iii) the battery can be assembled in the discharged state.

Further work is necessary to increase the stability of the graphite material and, hence, prolong cycle life. This can

be achieved by choosing suitable solvent systems such as mixtures of solvents, solvents with additives, solid polymer electrolyte systems, and gelled polymer electrolyte systems. Some work on these lines are in progress.

Acknowledgements

One of the authors (R.S.) would like to thank CSIR, New Delhi, for the award of a Research Associateship.

References

[1] J.M. Tarascon, D. Guyomard, Electrochim. Acta 38 (1992) 1221.
[2] J.O. Besenhard, H.P. Fritz, J. Electroanal. Chem. 53 (1974) 329.
[3] Y. Maeda, S. Harada, Synth. Met. 31 (1989) 389.
[4] D. Billaud, F.X. Henry, P. Willmann, Mat. Res. Bull. 28 (1993) 477.
[5] Z.X. Shu, R.S. MacMillan, J.J. Murray, J. Electrochem. Soc. 140 (1993) 922.
[6] D. Aurbach, Y. Ein-Eli, O. Chisid, Y. Carmeli, M. Babai, H. Yamin, J. Electrochem. Soc. 14 (1994) 603.
[7] R. Yazami, K. Zaghip, M. Deschamps, J. Power Sources 52 (1994) 55.
[8] T. Ohzuku, Z. Takekara, S. Yoshizawa, Denki Kagaku 46 (1978) 438.
[9] Y. Matsuda, M. Morita, H. Katsuma, Denki Kagaku 51 (1983) 744.
[10] F. Beck, H. Krohn, Synth. Met. 14 (1986) 137.
[11] R. Santhanam, M. Noel, J. Power Sources 63 (1996) 1.
[12] R. Santhanam, M. Noel, J. Power Sources 66 (1997) 47.
[13] M. Noel, R. Santhanam, M. Francisca Flora, J. Power Sources 56 (1995) 125.
[14] R.T. Carlin, H.C. De Long, J. Fuller, P.C. Truelove, J. Electrochem. Soc. 141 (1994) L73.
[15] R. Santhanam, M. Noel, J. Power Sources 56 (1996) 101.
[16] S. Panero, E. Spila, B. Scrosati, J. Electrochem. Soc. 143 (1996) L29.
[17] R. Santhanam, P. Kamaraj, M. Noel, J. Power Sources 72 (1998) 239.
[18] S. Mori, H. Asahina, H. Suzuki, A. Yonei, K. Yokoto, J. Power Sources 68 (1997) 59.
[19] D. Aurbach, A. Zaban, Y. Ein-Eli, I. Weissmann, O. Chusid, B. Markovsky, M. Levi, E. Levi, A. Schechter, E. Granot, J. Power Sources 68 (1997) 91.
[20] Y. Maeda, S. Harada, Synth. Met. 31 (1989) 389.
[21] D. Aurbach, Y. Ein-Eli, O. Chusid, Y. Carmeli, M. Babai, H. Yamin, J. Electrochem. Soc. 14 (1994) 603.